International Journal of Nanomedicine

Dovepress
open access to scientific and medical research

Open Access Full Text Article

ORIGINAL RESEARCH

Docetaxel-loaded solid lipid nanoparticles suppress breast cancer cells growth with reduced myelosuppression toxicity

This article was published in the following Dove Press journal:
International Journal of Nanomedicine
17 October 2014
Number of times this article has been viewed

Qing Yuan[1]
Jing Han[1,2]
Wenshu Cong[1]
Ying Ge[3]
Dandan Ma[1,3,4]
Zhaoxia Dai[3,4]
Yaping Li[5]
Xiaolin Bi[1,3,4]

[1]CAS Key Laboratory for Biological Effects of Nanomaterials and Nanosafety, Institute of High Energy Physics, Chinese Academy of Sciences, Beijing, [2]School of Life Sciences, Anhui University, Hefei, [3]Cancer Center, Institute of Cancer Stem Cell, Dalian Medical University, Dalian, [4]Graduate School, Dalian Medical University, Dalian, [5]Shanghai Institute of Materia Medica, Chinese Academy of Sciences, Shanghai, People's Republic of China

Abstract: Docetaxel is an adjuvant chemotherapy drug widely used to treat multiple solid tumors; however, its toxicity and side effects limit its clinical efficacy. Herein, docetaxel-loaded solid lipid nanoparticles (DSNs) were developed to reduce systemic toxicity of docetaxel while still keeping its anticancer activity. To evaluate its anticancer activity and toxicity, and to understand the molecular mechanisms of DSNs, different cellular, molecular, and whole genome transcription analysis approaches were utilized. The DSNs showed lower cytotoxicity compared with the commercial formulation of docetaxel (Taxotere®) and induced more apoptosis at 24 hours after treatment in vitro. DSNs can cause the treated cancer cells to arrest in the G2/M phase in a dose-dependent manner similar to Taxotere. They can also suppress tumor growth very effectively in a mice model with human xenograft breast cancer. Systemic analysis of gene expression profiles by microarray and subsequent verification experiments suggested that both DSNs and Taxotere regulate gene expression and gene function, including DNA replication, DNA damage response, cell proliferation, apoptosis, and cell cycle regulation. Some of these genes expressed differentially at the protein level although their messenger RNA expression level was similar under Taxotere and DSN treatment. Moreover, DSNs improved the main side effect of Taxotere by greatly lowering myelosuppression toxicity to bone marrow cells from mice. Taken together, these results expound the antitumor efficacy and the potential working mechanisms of DSNs in its anticancer activity and toxicity, which provide a theoretical foundation to develop and apply a more efficient docetaxel formulation to treat cancer patients.

Keywords: docetaxel, docetaxel-loaded solid lipid nanoparticles, breast cancer, toxicity

Introduction

Docetaxel is a widely used antitumor drug that is semi-synthesized from 10-deacetylbaccatin III, an inactive taxoid precursor prepared from needles of the European yew, *Taxus baccata*.[1] It has been used to treat a broad spectrum of solid tumors such as advanced ovarian cancer, non-small-cell lung cancer, locally advanced or metastatic breast cancer, and androgen-independent prostate cancer.[2–4] Docetaxel belongs to the taxane family that can promote assembly of free tubulin into microtubules and stabilize them by binding to tubulin to inhibit disassembly of microtubules.[5,6] Docetaxel suppresses tumor cell growth in two different modes: at high concentration, docetaxel induces G2/M cell cycle arrest and apoptosis, whereas a very low level of docetaxel causes aberrant mitosis followed by necrosis.[7,8] Although docetaxel has many advantages in cancer therapy, it can cause serious side effects, such as neutropenia, myelosuppression, anemia, and hypersensitivity reaction, which limit its clinical applications.[9–11] Some of these side effects are simply induced by

Correspondence: Yaping Li
Shanghai Institute of Materia Medica, Chinese Academy of Sciences, Shanghai 201203, People's Republic of China
Tel +86 21 5080 6820
Fax +86 21 5080 6820
Email ypli@simm.ac.cn

Xiaolin Bi
CAS Key Laboratory for Biological Effects of Nanomaterials and Nanosafety, Institute of High Energy Physics, Chinese Academy of Sciences, Beijing 100049, People's Republic of China
Tel +86 10 8823 6709
Fax +86 10 8823 6456
Email bixl@ihep.ac.cn

the formulation vehicles that are added to improve poor solubility of docetaxel, such as surfactant polysorbate 80.[12,13] To date, a lot of effort has been put into improving the formulation to simultaneously reduce its side effects and enhance its antitumor activity. With the progress of nanotechnology and its applications in medicine, nanoparticle drug delivery systems can revive the clinical potential of abandoned compounds by reducing their toxicity.[14] Recently, many new solvent-free formulations of docetaxel, such as chitosan nanoparticles, solid lipid nanoparticles, or poly(lactide-co-glycolide) nanoparticles,[15–17] emulsions,[18] liposomes,[19–21] targeted lipid-polymer,[22] and micelles,[23–25] were developed and used to reduce the side effects and improve the therapeutic effect. These nanotechnology-based formulations exhibit good prospects to reduce toxicity, increase the maximum tolerated dose,[26] and reduce the mean body weight loss,[27] as well as lower severe anemia and liver damage in mice.[28]

The authors' previous work showed that docetaxel-loaded solid lipid nanoparticles (DSNs) have many advantages compared with other nanoformulations, including easier preparation, better stability, component materials safety, and controlled release.[29,30] The authors have performed systemic analysis of DSN toxicity, including acute toxicity, irritation, allergenicity, and long-term toxicity, using different animal models.[29] Compared with commercially available formulations of docetaxel (Taxotere® [TAX]), DSNs have lowered hemotoxicity, hepatotoxicity, and myelotoxicity.[29] In addition, DSNs increase the maximum tolerated dose of TAX, reduce the inherent toxicity, and prevent the associated anaphylaxis induced by polysorbate 80.[29]

Breast cancer is one of the most common malignant tumors and the most significant cause of mortality among women around the world.[31,32] For early, high-risk, and metastatic breast cancer patients, docetaxel is one of the most effective drugs for adjuvant therapy.[4,33] In the present work, the antibreast cancer activity and toxicity of newly formulated DSNs were evaluated both in vitro and in vivo. Moreover, the potential molecular mechanisms in tumor suppression and toxicity reduction were investigated by gene expression profiles and different cellular and molecular approaches.

Materials and methods

Drugs

Docetaxel was purchased from Shenzhen Main Luck Pharmaceuticals Inc., (Shenzhen, People's Republic of China). DSNs and blank solid lipid nanoparticles (BSNs) were prepared at the Shanghai Institute of Materia Medica, Chinese Academy of Sciences (Shanghai, People's Republic of China).

Preparation and characterization of DSNs

DSNs were prepared by the high-pressure homogenization method, as described previously.[29] Briefly, a mixture of docetaxel/soybean lecithin/trimyristin (1:5:15, w/w) was dissolved in ethanol, added to preheated water (65°C) under agitation, and sonicated to form the oil-in-water emulsions. Then, the emulsions were homogenized with a high-pressure homogenizer (EmulsiFlex-C3; Avestin, Inc., Ottawa, ON, Canada) for three cycles at 20,000 psi to form the DSNs. The BSNs were prepared using the same procedure. Thereafter, the DSN suspension was lyophilized and stored at 4°C for further measurements. The size distribution and ζ potential values of DSNs were measured by dynamic light scattering (Nicomp 380 ZLS; Particle Sizing Systems, Port Richey, FL, USA). The morphology of DSNs was observed by a transmission electron microscope (CM12; Philips NV, Amsterdam, the Netherlands). The encapsulation efficiency of docetaxel in the DSNs was determined by high-performance liquid chromatography quantification, as described previously (Agilent 1100; Agilent Technologies, Santa Clara, CA, USA).[29]

Cell cytotoxicity assay

Cells were obtained from American Type Culture Collection (Rockville, MD, USA). The cytotoxicity of TAX, DSNs, and BSNs was evaluated by Cell Counting Kit-8 system (Dojindo Laboratory, Kumamoto, Japan). Cells were seeded into 96-well plates at the density of 5×10^3 cells in 100 μL complete Dulbecco's Modified Eagle Medium (DMEM) per well. After being cultured for 24 hours, cells were treated with different doses of DSNs (0–100 nM) or equivalent TAX for 24 hours, 48 hours, and 72 hours. Equivalent BSNs were used as the control. After cells were treated for the indicated time, Cell Counting Kit-8 was added and incubated for 1 hour at 37°C. Absorbance was measured at 450 nM with a SpectraMax® M2 microplate reader (Molecular Devices, Sunnyvale, CA, USA). The cell viability was calculated and shown as the mean ± standard error of triplicate experiments.

Apoptosis assay

Apoptosis was detected by an Accuri™ C6 flow cytometer (BD, Franklin Lakes, NJ, USA) after staining with Annexin V-Fluorescein Isothiocyanate Apoptosis Detection Kit I (BD Biosciences, San Jose, CA, USA) according to the manufacturer's instructions. Fifty thousand cells were cultured for 24 hours and

treated with different doses of TAX and DSNs (0–100 nM) for 24 or 48 hours. Cells were stained with Annexin V-fluorescein isothiocyanate and propidium iodide; the percentage of apoptotic cells was quantified by fluorescence-activated cell sorting analysis. At least 20,000 cells were analyzed for each sample; CFlow Plus (BD) was used to analyze the results.

Cell cycle profile detection

The cell cycle profile was detected with an Accuri C6 flow cytometer (BD) by using a Cell Cycle and Apoptosis Analysis Kit (Beyotime Institute of Biotechnology, Haimen, People's Republic of China) following the manufacturer's instructions. Cells were seeded into 24-well plates at 5×10^4 cells/well and cultured for 24 hours. Then, cells were treated with different doses of TAX, DSNs, and BSNs (0–100 nM) in DMEM supplied with 10% fetal bovine serum (FBS) for 24 or 48 hours. After treatment, cells were fixed with 70% (v/v) cold ethanol overnight and stained with propidium iodide. The cell cycle profile was analyzed by fluorescence-activated cell sorting analysis; at least 20,000 cells were analyzed for each sample.

In vivo tumor suppression test

The tumor suppression effects of DSNs and TAX were investigated with tumor-bearing female BALB/c nude mice in the JOINN Laboratories (Beijing, People's Republic of China). BALB/c nude mice were purchased from Vital River Laboratories (Beijing, People's Republic of China). Mice were subcutaneously injected with MCF-7 cells. After 3 weeks, the tumor-bearing mice were sacrificed and the tumor tissues were isolated and cut into pieces of about 2 mm^3 under aseptic conditions. Around 4–5 week-old mice were subcutaneously inoculated with tumor tissue in the right flank. Tumors were allowed to grow to about 50–100 mm^3. Mice bearing a similar tumor volume were chosen and randomly divided into four groups, with six mice in each group. Mice from different groups were treated with 10 mg/kg of TAX, DSNs, equivalent BSNs, or glucose (GLU) separately by tail vein injection every 4 days. Body weight and tumor size were measured every 3 days. Mice were sacrificed on Day 12 and tumor tissues were isolated and frozen in liquid nitrogen immediately for future studies. Tumor volume was calculated as one-half of the product of the three orthogonal diameters. Relative tumor volume (RTV) was calculated as the volume on a specific day after drug treatment divided by the initial volume before treatment.

Microarray assay and data analysis

Total RNA was isolated from frozen tumor samples and hybridized to Affymetrix Human Genome U133 Plus 2.0 Array by CapitalBio Corporation (Beijing, People's Republic of China) according to the Affymetrix GeneChip® Expression Analysis Technical Manual. The GeneChip contains 47,000 transcripts corresponding to 38,500 confirmed human genes. The expression raw data was preprocessed using robust multichip analysis with quantile normalization and custom CDF file hgu133plus2hsentrezgcdf, version 17.1.0.[34] A limma linear model with empirical Bayes moderation was applied for differentially expressed gene calling.[35] The adjusted *P*-value for significance cutoff was 0.05, and the fold change cutoff was 1.5. Differentially expressed genes were cluster ordered on the basis of their correlations (average linkage, Spearman's rank correlation), with hierarchical clustering. Gene enrichment analysis of annotation terms was performed using the Database for Annotation, Visualization, and Integrated Discovery (DAVID) functional annotation program.[36] The microarray data from this study have been submitted to the NCBI Gene Expression Omnibus (http://www.ncbi.nlm.nih.gov/geo/) under accession number GSE54091.

Quantitative polymerase chain reaction (qPCR)

The qPCR was performed with iQ™5 Multicolor Real-Time PCR Detection System (Bio-Rad Laboratories, Inc., Hercules, CA, USA) according to the manufacturer's recommendations. The total RNA used was the same as that used in the microarray assay and purified with RNeasy Plus Mini Kit (Qiagen NV, Venlo, the Netherlands). Purified RNA was reverse transcribed into complementary DNA by using an $Oligo(dT)_{15}$ Primer (Promega Corporation, Fitchburg, WI, USA) and M-MLV Reverse Transcriptase (Promega) following the manufacturer's instructions. The qPCR was performed with iQ SYBR® Green Supermix (Bio-Rad) with standard protocol. Sequences of the primers were obtained from PrimerBank (http://pga.mgh.harvard.edu/primerbank/index.html) and OligoArchitect™ Online tools v3.0 (Sigma-Aldrich Co., St Louis, MO, USA), and the optimal primer pairs were verified by regular PCR. The amplification factor was calculated by the comparative threshold cycle method. β-actin was used as the internal control.

Immunoblotting

Proteins were detected by standard immunoblotting protocol. Frozen tumor tissues were homogenized with a mortar and pestle in liquid nitrogen, then the powder was lysed with radioimmunoprecipitation assay buffer (50 mM Tris HCl, pH 7.4, 150 mM NaCl, 1% Triton X-100, 1% sodium deoxycholate, 0.1% sodium dodecyl sulfate, 1 mM sodium orthovanadate,

50 mM NaF, and 1mM ethylenediaminetetraacetic acid) containing a protease inhibitor cocktail tablet (Hoffman-La Roche Ltd., Basel, Switzerland) for 20 minutes at 4°C. Loading buffer was added and samples were denatured for 5 minutes at 95°C. Samples of equal amounts were subjected to 10% sodium dodecyl sulfate polyacrylamide gel electrophoresis and transferred to polyvinylidene fluoride membranes. Primary antibodies of rabbit anti-β-actin, E2f8, MRE11A, ERBB3, IGFBP6, ATF3, CCNG2, SOD2, IGFBP3, CADM1, PDCD4, GADD45A, and MKI67 were purchased from Beijing Biosynthesis Technology Co., Ltd., (Beijing, People's Republic of China), rabbit anti-MCM6, OIP5, and NASP were purchased from Proteintech Group, Inc., (Chicago, IL, USA), rabbit anti-FAM172A and MYB were purchased from Abgent, Inc. (San Diego, CA, USA) and rabbit anti-ATRX was purchased from GeneTex, Inc. (Irvine, CA, USA). The primary antibodies were diluted at 1:1,000. Horseradish peroxidase-conjugated goat anti-rabbit secondary antibody (1:5,000; Jackson ImmunoResearch Laboratories, Inc., West Grove, PA, USA) was used. Antibody/antigen reactions were visualized by Amersham™ ECL™ Prime Western Blotting Detection Reagent (GE Healthcare UK Ltd., Little Chalfont, UK).

Hematopoietic colony-forming cell (CFC) assay

The hematopoietic CFC assay of primary mouse bone marrow cells was performed in MethoCult™ Methylcellulose-Based Medium (STEMCELL Technologies Inc., Vancouver, BC, Canada) following the manufacturer's instructions. The animal experiments were performed in compliance with the local ethics committee. Two 7-week-old BALB/C mice were sacrificed in each test using procedures recommended by the Institutional Animal Care and Use Committee. Bone marrow cells were isolated from the tibias right after animals were sacrificed with cold Iscove's Modified Dulbecco's Medium containing 2% FBS. Cells were diluted in 3% acetic acid with methylene blue and total nuclei were counted with a hemocytometer. Cells were suspended in 50 μL Iscove's Modified Dulbecco's Medium containing 2% FBS and plated on a 24-well plate at 4×10^4 cells/well. Then, 450 μL MethoCult medium was added and drugs at the indicated concentrations were added and mixed well. Medium- and BSN-treated groups were used as the controls. Two doses (3 nM and 6 nM) of DSNs and TAX were evaluated; each treatment was repeated in three wells each time and the whole test was performed for triplicated. Cells were incubated at 37°C and 5% CO_2 for about 9 days until colonies of burst-forming units that generate erythroids (BFU-E), colony forming units that generate granulocytes, erythroids, macrophages, and megakaryocytes (CFU-GEMM), and colony forming units that generate granulocytes and macrophages (CFU-GM) were formed and numbers were counted.

Statistical analysis

Statistical analyses were performed with Student's *t*-test. Levene's test, analysis of variance, Dunnett's test, Kruskal–Wallis test, and Mann–Whitney *U*-test were used in the animal tests.

Results

Preparation and characterization of DSNs

DSNs were prepared with a conventional high-pressure homogenization method. The DSNs were round and uniform as observed by transmission electron microscopy (Figure S1). The mean diameter of the DSNs was 37.17±0.35 nm and the polydispersity index was 0.258±0.030, which was in accordance with the transmission electron microscope measurements. In addition, the ζ potential of the DSNs was –28.1±3.53 MV. The encapsulation efficiency of DSNs was 91.77%±1.75%, which implicates the high encapsulation of docetaxel in the solid lipid nanoparticles.

Cytotoxicity of DSNs and TAX in MCF-7 cells

Previous studies have shown that TAX can suppress the growth of MCF-7 breast cancer cells, and have used MCF-7 cells to study its mechanisms.[7,8] To explore whether DSNs have a similar tumor suppression effect to TAX, MCF-7 cells were treated with different doses of DSNs and TAX as well as BSNs for 24, 48, and 72 hours, respectively. Complete DMEM with 10% FBS was used as the control. For each drug used, different doses from 1 nM–100 nM were tested. After treatment for the indicated duration and concentration, cell viability was explored by Cell Counting Kit-8 assay.[37] Cell growth was greatly suppressed by DSNs and TAX in a dose- and time-dependent manner, although BSNs did not show an obvious growth suppression effect compared with the DMEM control at every dose and time point tested (Figure 1). The cytotoxicity of DSNs was compared with TAX at each dose at indicated time points. After treatment for 24 hours, the percentage of viable cells in the DSN- or TAX-treated group showed no significant difference at every dose used (Figure 1A; $P>0.05$). However, DSNs showed significant lower cytotoxicity in MCF-7 cells compared

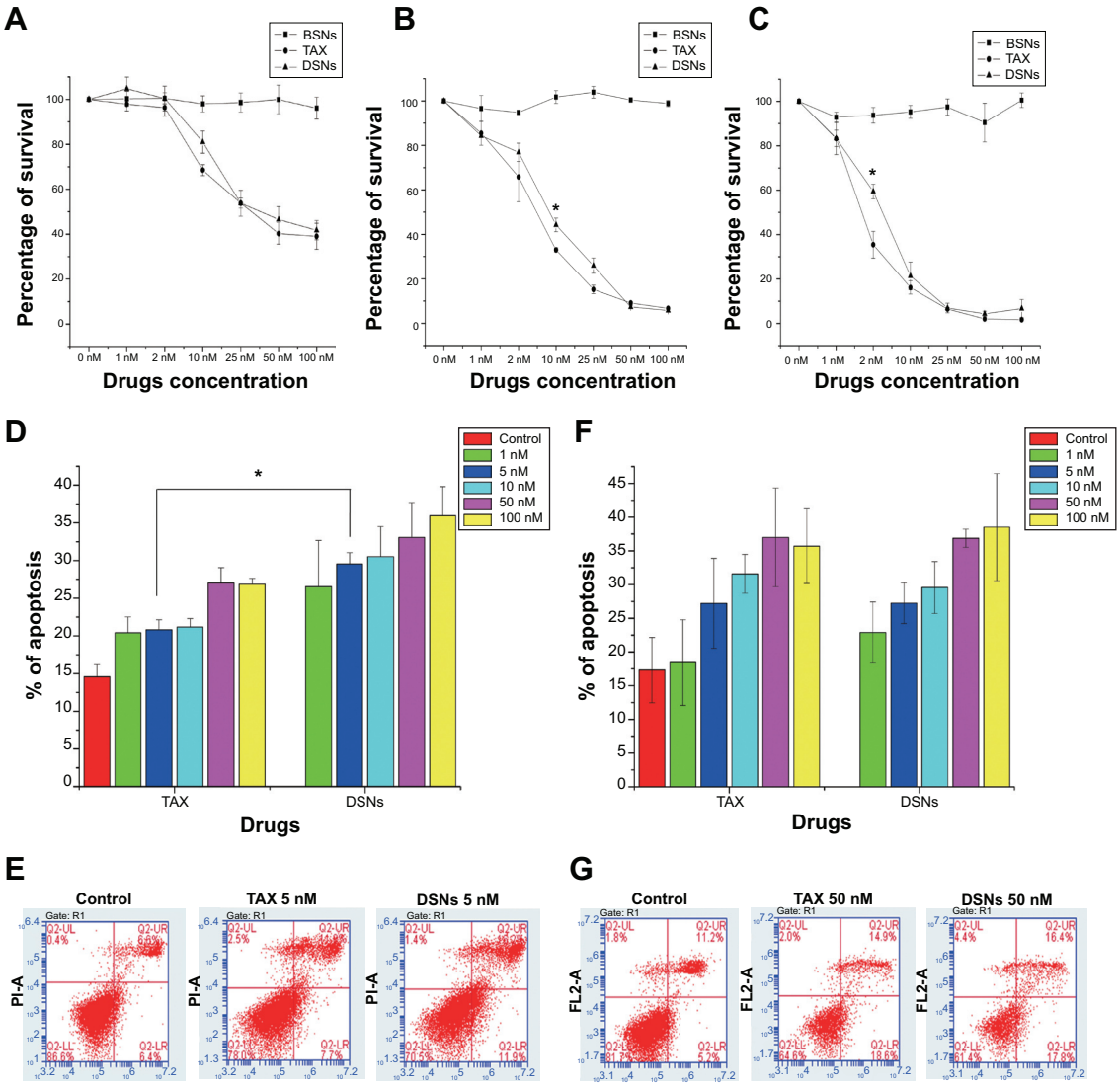

Figure 1 Docetaxel-loaded solid lipid nanoparticles inhibit growth and induce apoptosis in human MCF-7 cancer cells.

Notes: MCF-7 cells were treated with 1–100 nM docetaxel-loaded solid lipid nanoparticles or Taxotere® for 24 hours (**A**, **D**, **E**), 48 hours (**B**, **F**, **G**), and 72 hours (**C**), respectively. Cell viability was quantified (**A**–**C**). Apoptosis was determined at 24 hours (**D**) and 48 hours (**F**). Fluorescence-activated cell sorting results of the 5 nM dose for 24 hours (**E**) and the 50 nM dose for 48 hours (**G**). The lower right quadrant and upper right quadrant represent the percentage of early apoptotic cells and late apoptotic cells, respectively. Data are presented as mean ± standard error from three experiments. *$P<0.05$.

Abbreviations: BSN, blank solid lipid nanoparticle; DSN, docetaxel-loaded solid lipid nanoparticle; LL, lower left; LR, lower right; TAX, Taxotere; UL, upper left; UR, upper right.

with TAX at doses of 10 nM after 48-hours of treatment and 2 nM after 72-hours of treatment, respectively (Figure 1B and C; $P<0.05$). These data suggest that both DSNs and TAX strongly suppress the growth of MCF-7 breast cancer cells. The data also suggests that the suppression effect of DSNs is not from the nanoparticle carrier, as BSNs do not show any suppression effect in vitro.

Apoptosis induced by DSNs and TAX in MCF-7 cells

Most antitumor drugs can suppress tumor cell growth by inducing apoptosis. To explore whether DSNs and TAX also induced apoptosis, MCF-7 cells were stained with Annexin V-fluorescein isothiocyanate and propidium iodide after treatment with DSNs and TAX. Cells were incubated with 1 nM, 5 nM, 10 nM, 50 nM, and 100 nM DSNs and TAX for 24 and 48 hours, respectively. Then, apoptotic cells were detected by flow cytometry. Results from three independent experiments showed that both DSNs and TAX induced apoptosis, including both early apoptosis and late apoptosis in a dose- and time-dependent manner, while a very low level of apoptosis was detected in the control samples (Figure 1). Moreover, there was no significant difference between the percentage of total apoptosis with DSN and TAX treatment

at the same dose and time points except for 24-hour treatment with the 5 nM dose (Figure 1; $P>0.05$). When MCF-7 cells were treated with 5 nM DSNs and TAX for 24 hours, the percentage of apoptotic cells was 29.6%±1.5% versus 20.8%±1.3%, respectively, which shows a significant difference (Figure 1D and E; $P<0.05$). DSN- and TAX-induced apoptosis was also demonstrated by morphological changes of treated cells detected under a microscope, and these results were consistent with that of flow cytometry (Figure S2). All these data suggest that both DSNs and TAX induce apoptosis in MCF-7 cells, and DSNs are more efficient compared with TAX when treated for 24 hours at the 5 nM dose after 24-hour treatment.

Cell cycle profiles after DSN and TAX treatment

As docetaxel causes aberrant mitosis and impairs proliferation of tumor cells by stabilizing the microtubules, it was further tested whether DSNs and TAX induce cell cycle arrest. Cell cycle profiles were analyzed by flow cytometry after propidium iodide staining. Consistent with previous results,[7,8] most cells were arrested at the G2/M phase after TAX treatment in a dose-dependent manner (Figure 2). The percentage of G2/M phase cells was as high as 82.11%±1.76% when cells were treated with 100 nM TAX for 24 hours compared with 23.55%±3.93% in non-treated control samples (Figure 2A and B). When cells

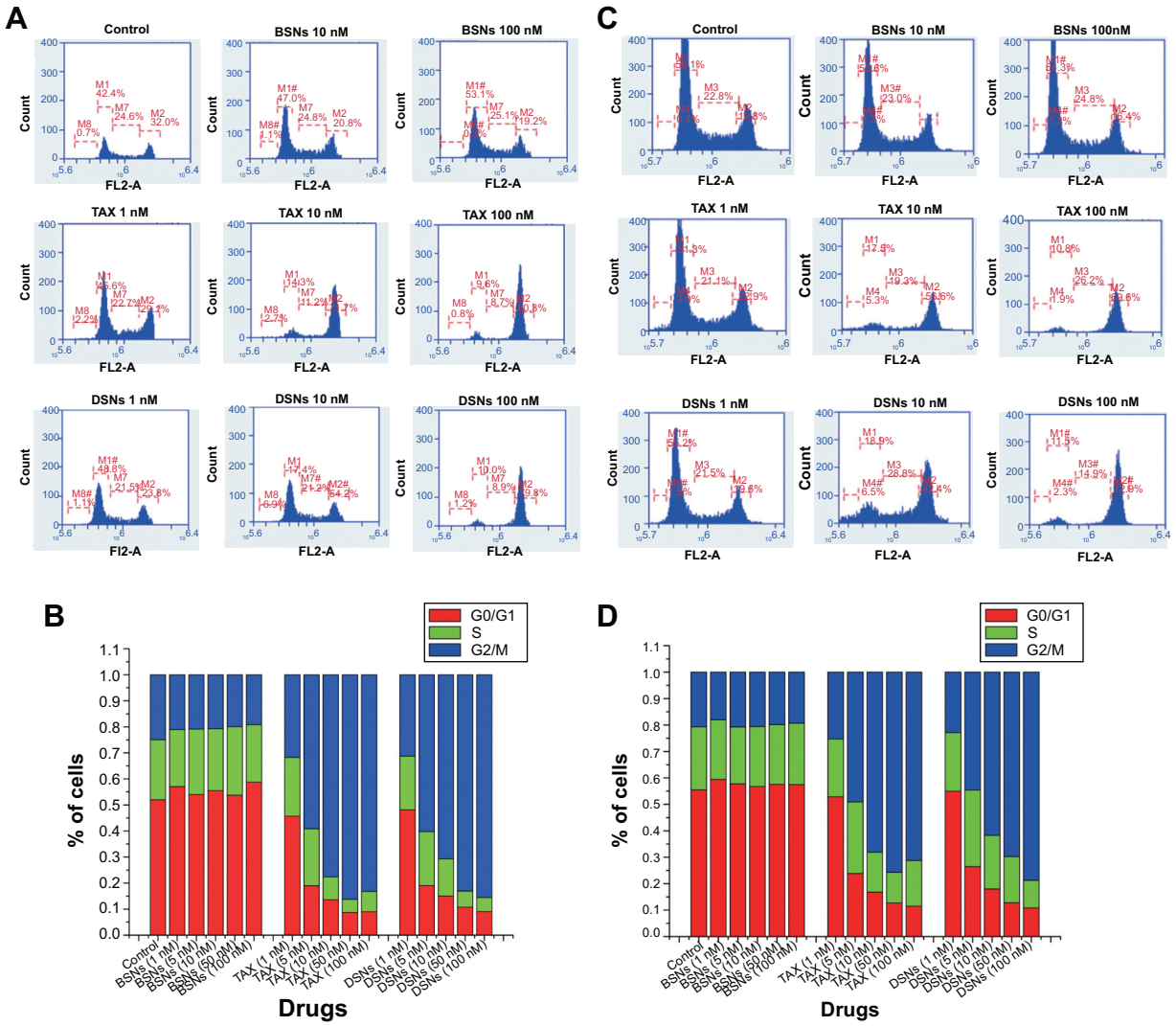

Figure 2 Docetaxel-loaded solid lipid nanoparticles induce G2/M cell cycle arrest in MCF-7 cells.

Notes: Cells were mock treated or treated with 1–100 nM docetaxel-loaded solid lipid nanoparticles, Taxotere®, or blank solid lipid nanoparticles for 24 hours (**A**, **B**) and 48 hours (**C**, **D**), respectively. Cells were fixed and stained with propidium iodide for cell cycle phase distribution analysis. Representative flow cytometry profiles of the cell cycle phase distribution of MCF-7 cells after treatment for 24 hours (**A**) and 48 hours (**C**). The first peak indicates 2n DNA content in the G0/G1 phase, the second peak indicates 4n DNA content in the G2/M phase, and in-between the two peaks is the S phase. Cell cycle phase distribution of MCF-7 cells after treatment for 24 hours (**B**) and 48 hours (**D**). Data are presented as mean ± standard error from three experiments.

Abbreviations: BSN, blank solid lipid nanoparticle; DSN, docetaxel-loaded solid lipid nanoparticle; TAX, Taxotere.

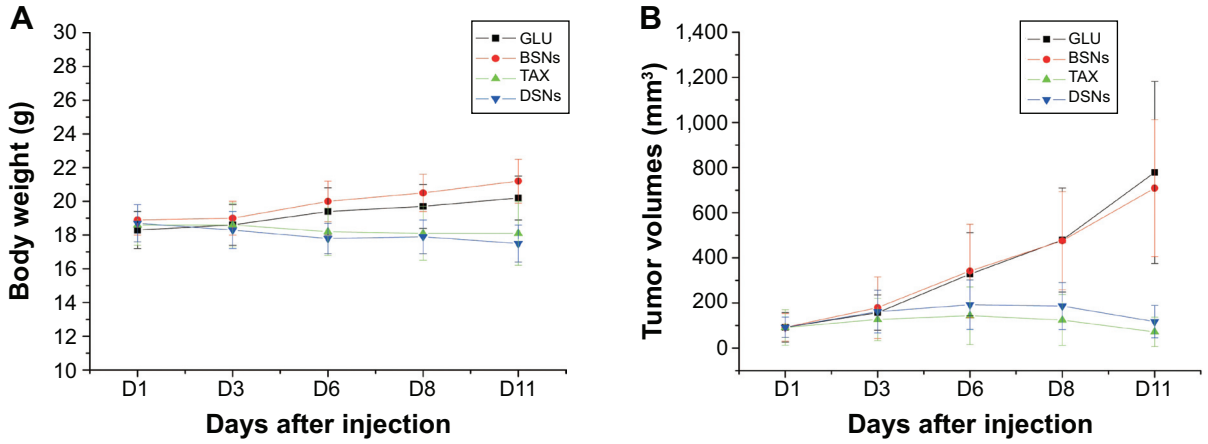

Figure 3 Body weight changes of tumor-bearing mice and the antitumor effect of docetaxel-loaded solid lipid nanoparticles and Taxotere®.
Notes: Tumor-bearing mice were treated with 10 mg/kg docetaxel-loaded solid lipid nanoparticles or Taxotere. Their body weight was measured at the indicated days and the mean weight of each group is shown (**A**). An equal amount of blank solid lipid nanoparticles and glucose was set as the control. The tumor volume was measured at the indicated days and the mean volume of each group is shown (**B**).
Abbreviations: BSN, blank solid lipid nanoparticle; DSN, docetaxel-loaded solid lipid nanoparticle; GLU, glucose; TAX, Taxotere.

were treated with 100 nM TAX for 48 hours, the percentage of G2/M phase cells was 70.98%±1.39% compared with 19.83%±2.1% in mock-treated cells (Figure 2C and D). The cell cycle distribution in the DSN-treated group was almost the same as that of the TAX-treated group at every dose tested (Figure 2). The percentage of G2/M phase cells was 83.8%±3.97% and 78.51%±5.64% when treated with 100 nM DSNs for 24 and 48 hours, respectively (Figure 2B and D). These data suggest that DSNs still cause cell cycle arrest like TAX, which provides further evidence for potential clinical applications of DSNs.

Tumor suppression of DSNs and TAX in vivo

To explore whether DSNs can be used to treat tumors in vivo, the tumor suppression effect of DSNs and TAX was investigated in tumor transplantation nude mice. BALB/c nude mice were subcutaneously injected with MCF-7 cells and tumors were formed after about 3 weeks. The tumor tissue was isolated and cut into almost equal-sized pieces under aseptic conditions and subcutaneously inoculated into the axilla of nude mice. Tumor-bearing mice were randomly divided into four groups, with six mice in each group. The mice in each group were treated with GLU, BSNs, TAX, or DSNs separately by tail vein injection. The drug dose was 10 mg/kg animal weight and the injection was performed every 4 days. Body weight and tumor size were measured every 3 days until the mice were sacrificed. In the GLU-treated group, the mice gained body weight regularly and the mean tumor volume increased gradually (Figure 3). On Day 11, the day before the mice were sacrificed, the mean tumor volume in the GLU group was 9.45-fold greater than before treatment, and RTV was 9.45±3.43 (Figure 3B; Table 1). In the BSN-treated group, the mice also gained body weight regularly and the RTV on Day 11 was 8.85±2.40; both body weight and RTV were not significantly different compared with the GLU-treated group (Figure 3; Table 1; $P>0.05$). These data suggest that BSNs do not cause any potential toxicity in tumor-bearing mice and have no tumor suppression effect by itself. Compared with the control groups, the body weight of TAX- and DSN-treated mice decreased gradually, while RTV was reduced significantly in both groups (0.76±0.34 in the TAX-treated group and 1.37±1.05 in the DSN-treated group) (Figure 3; Table 1; $P<0.01$); however,

Table 1 Antitumor efficiency of docetaxel-loaded solid lipid nanoparticles and Taxotere® in vivo

Treatment	Dose (mg/kg)	Mice (n)	D3	D6	D8	D11
GLU	–	6	1.87±0.31	4.02±1.36	5.96±2.26	9.45±3.43
BSNs	10	6	1.84±0.25	3.83±0.27	5.92±1.58	8.85±2.40
TAX	10	6	1.57±0.40	1.71±0.82***	1.48±0.67**	0.76±0.34**
DSNs	10	6	1.74±0.28	2.11±0.89**	2.12±1.27**	1.37±1.05**

Notes: Data show relative tumor volume compared with GLU group. **$P\leq0.01$. ***$P\leq0.001$.
Abbreviations: BSN, blank solid lipid nanoparticle; D, day; DSN, docetaxel-loaded solid lipid nanoparticle; GLU, glucose; TAX, Taxotere.

there was no significant difference between the TAX- and DSN-treated groups ($P>0.05$). These results suggest that DSNs can inhibit MCF-7 breast cancer growth effectively in vivo at a dose of 10 mg/kg, implicating a similar potential clinical application as TAX.

Genes influenced by TAX and DSNs at the transcription level in tumor tissue

To understand the mechanisms by which TAX and DSNs suppress tumor growth, the gene expression profiles were systemically analyzed at the transcription level by complementary DNA microarrays. Tumor tissue was obtained from tumor-bearing mice after treatment with GLU, BSNs, TAX, or DSNs. Total RNA was extracted from the tumor tissue and Affymetrix GeneChip Human Genome U133 Plus 2.0 messenger RNA microarray, which includes 54,614 probes for 47,000 transcripts of 18,898 human Entrez genes, was used to detect transcripts of human genes. The gene expression profile after TAX, DSN, or BSN treatment was compared with the GLU-treated control. The gene expression profile between TAX and DSN treatment was also compared. Genes with a 1.5 fold change (adjusted $P<0.05$), either upregulated or downregulated, were recognized as significant and chosen for clustering (Table S1). As a safe and simple component material, BSNs showed no significant difference in the gene transcription profile compared with GLU, although the cutoff was as low as adjusted $P<0.05$ and fold change >1.5 (data not shown). Genes upregulated by TAX and DSNs are mainly involved in secrete and signal peptide coding, negative regulation of cell proliferation, and regulation of cell death (Figure 4A, Group 1; Table S1), and genes downregulated by TAX and DSNs are mainly involved in DNA replication, DNA damage response, and the cell cycle process (Figure 4A, Group 2; Table S1). Compared with BSNs and GLU treatment, TAX induced 135 upregulated genes and 489 downregulated genes, DSNs induced 53 upregulated genes and 106 downregulated genes (Figure 4B; Table S1). Genes up- or downregulated by DSN treatment mostly overlapped with the TAX-treated group, with 49 upregulated genes and 98 downregulated genes in common (Figure 4B; Table S1). As TAX and DSNs have the same functions to induce apoptosis, arrest cell cycle at the G2/M stage, and suppress tumor growth in vivo, the microarray results provide further evidence that TAX and DSNs are working similarly both towards intrinsic mechanisms and antitumor therapy. The microarray data from this study have been submitted to the NCBI Gene Expression Omnibus under accession number GSE54091.

To verify the microarray assay results, qPCR experiments were performed. Twenty-seven potential genes were investigated (Table S2). The qPCR results showed that 21 genes were expressed at the same level as detected by microarray assay (Table 2; Figure 5; Figure S3), and these genes have functions in the cell cycle, apoptosis, DNA damage response, and proliferation – with the only exception being *SMC1A*, which is involved in the cell cycle. The five genes that were inconsistent do not have functions in the cell cycle, apoptosis, DNA damage, or proliferation.

Protein expression regulated by TAX and DSNs

This study has shown that DSNs and TAX can influence cell proliferation, apoptosis, and the cell cycle. To investigate whether the protein expression of genes involved in these functions was also altered after DSN and TAX treatment, the protein expression of 18 genes that were verified by qPCR and involved in proliferation, apoptosis, the cell cycle, and DNA damage response were detected. Proteins were extracted from the same tumor tissue used in the messenger RNA experiments and detected with standard protocol. Compared with the GLU-treated group, the BSN-treated group did not cause any significant difference in protein expression level, which is consistent with the transcription level (Figure 5; Figure S4). In the TAX- and DSN-treated groups, 14 genes showed the same trend of protein expression as that of transcription. Surprisingly, four proteins showed the opposite trend to transcription (Figure 5; Figure S4). Moreover, one obvious difference between the TAX- and DSN-treated groups was observed. Although these 14 genes were expressed at a similar transcription level in both groups, 12 of them had different protein expression compared with transcription. These genes were: ERBB3, FAM172A, MKI67, and NASP – involved in proliferation regulation; E2F8, CCNG2, MCM6, and OIP5 – involved in cell cycle regulation; MRE11, ATRX, and MYB – involved in DNA damage response; and IGFBP3 – involved in apoptosis (Figure 5; Figure S4). Only SOD2 and PDCD4 had an equal protein expression and transcription level (Figure 5). SOD2 and PDCD4 have multiple functions in double-strand break repair, cell apoptosis, proliferation, and regulation of progression through the cell cycle. These data suggest that DSNs not only induce gene expression at the transcription level like TAX but also influence protein expression, and some proteins were expressed at a different level. The different expression of these proteins might be the reason that DSNs and TAX show different anticancer activity and reduced toxicity, which needs further investigation.

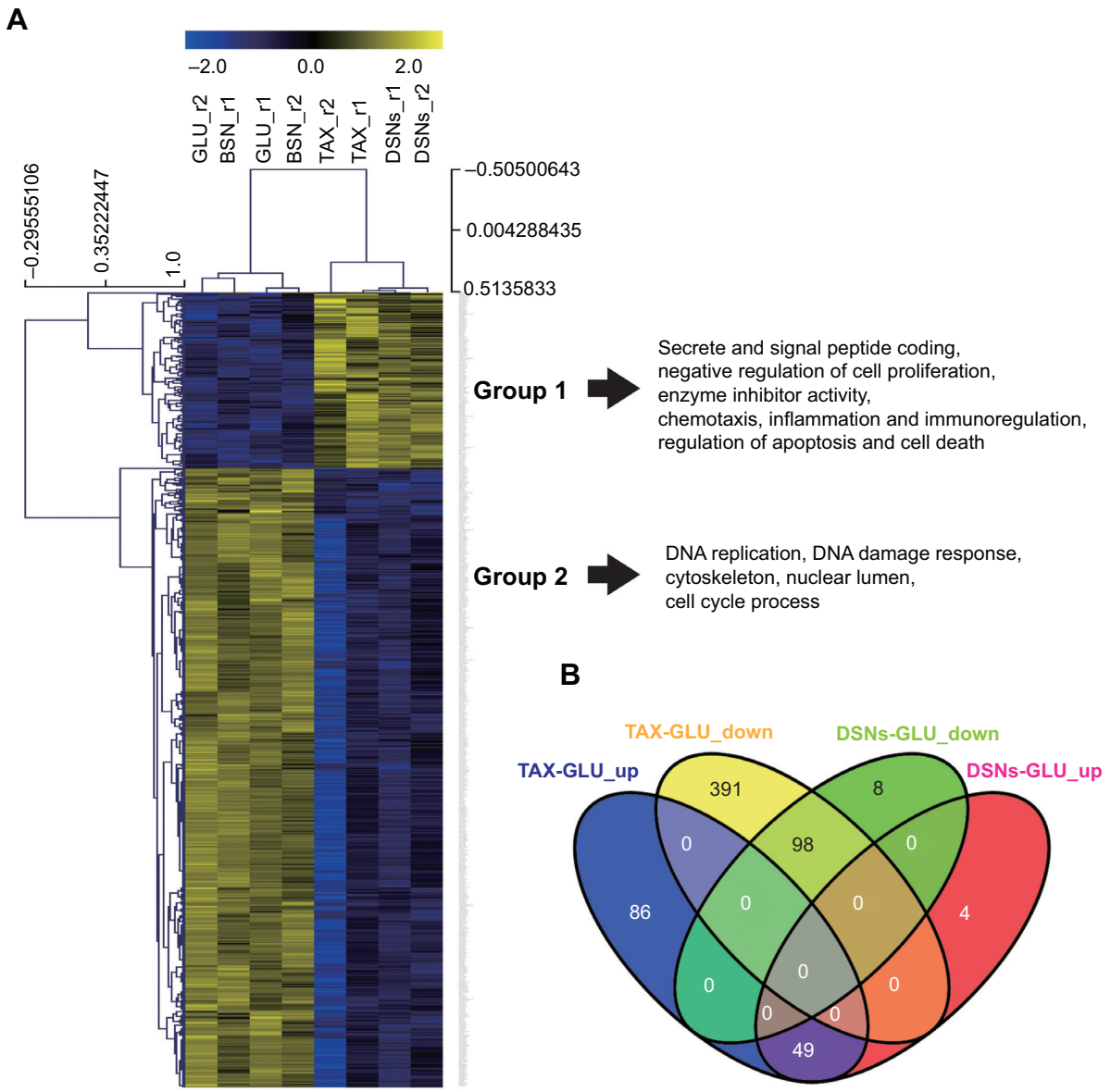

Figure 4 The union of differentially expressed genes in MCF7 cells when treated with glucose, Taxotere®, and docetaxel-loaded solid lipid nanoparticles.
Notes: Differentially expressed genes (adjusted $P<0.05$; fold change >1.5) were clustered into two groups, following functional annotation and enrichment analysis in each group. Each row represents one Entrez Gene, and the color scheme shows a normalized log2 gene expression index (**A**). The Venn diagram shows the common and differentially expressed genes under Taxotere and docetaxel-loaded solid lipid nanoparticles when compared with glucose (**B**).
Abbreviations: BSN, blank solid lipid nanoparticle; down, downregulated; DSN, docetaxel-loaded solid lipid nanoparticle; GLU, glucose; TAX, Taxotere; up, upregulated.

Myelosuppression of TAX and DSNs

TAX causes serious side effects when used clinically, and myelosuppression is one of the major side effects. In the authors' previous study, it was shown that the proliferation of bone marrow cells and the number of granulocytes were significantly reduced by TAX treatment in beagle dogs, whereas DSNs reduced TAX-induced bone marrow cytotoxicity by increasing proliferation of the bone marrow cells.[29] Besides the increased proliferation of bone marrow cells, it was expected that the reduced cytotoxicity could be due to an increased number of mature cells from bone marrow primogenitor cells. To investigate this possibility, hematopoietic CFC assays were performed with primary mouse bone marrow cells in methylcellulose semi-solid medium containing DSNs or TAX to evaluate their myelosuppression toxicity.[38] Primary mouse bone marrow cells were isolated from the tibias of 7-week-old BALB/C mice[38] and cultured in methylcellulose-based medium. The cells were then treated with 3 nM or 6 nM DSNs or TAX for 9 days, and CFUs, including erythroid progenitors (BFU-Es) (made up of erythroid clusters and a minimum of 30 cells), CFU-GMs (the colonies contained 30 to thousands of granulocytes, macrophages, or

Table 2 Downregulated (↓) and upregulated (↑) genes in the Taxotere®- and docetaxel-loaded solid lipid nanoparticle-treated groups

	TAX	qPCR	DSNs	qPCR
↑	IGFBP6[$]	✓	IGFBP6[$]	✓
	ATF3	✓	ATF3	✓
	SOD2[$]	✓	SOD2[$]	✓
	CADM1[†‡]	✓	CADM1[†‡]	✓
	GLS		GLS	
	MAF		MAF	
	GADD45A[†‡]	✓	GADD45A[†‡]	✓
↓	BCL2L11		BCL2L11	
	PIK3R2[‡]		PIK3R2[‡]	
	E2F8[†]	✓	E2F8[†]	✓
	MRE11[#]	✓	MRE11[#]	✓
	HOXA13[‡]	✓	HOXA13[‡]	✓
	ERBB3[$]	✓	ERBB3[$]	✓
	FZD10	✓	FZD10	✓
	CCNG2[†]	✓	CCNG2[†]	✓
	ATRX[#]	✓	ATRX[#]	✓
	IGFBP3[‡]	✓	IGFBP3[‡]	✓
	SMC1A[†]		SMC1A[†]	
	C6ORF108[$]	✓	C6ORF108[$]	✓
	EHMT1		EHMT1	
	MCM6[†]	✓	MCM6[†]	✓
	FAM172A	✓	FAM172A	✓
	MYB	✓	MYB	✓
	PDCD4[†‡]	✓	PDCD4[†‡]	✓
	OIP5[†]	✓	OIP5[†]	✓
	MKI67[†$]	✓	MKI67[†$]	✓
	NASP[†$]	✓	NASP[†$]	✓

Notes: [†]Cell cycle-related genes. [‡]Apoptosis-related genes. [#]DNA damage response genes. [$]Proliferation-related genes. ✓ indicates that these genes were detected by qPCR and the results were consistent with microarray data.
Abbreviations: DSN, docetaxel-loaded solid lipid nanoparticle; qPCR, quantitative polymerase chain reaction; TAX, Taxotere.

both cell types), and CFU-GEMMs (which tend to produce large colonies of >500 cells containing erythroblasts and recognizable cells of at least two other lineages), were counted. Compared with mock-treated cells, the number of CFU-GMs did not change significantly in the 3 nM BSN-, DSN-, and TAX-treated groups (Figure 6B; 88.33±4.51 in the GLU-treated control group, 78±7.81 in the BSN-treated group, 78.33±5.13 in the DSN-treated group, and 73.33±9.29 in the TAX-treated group), whereas 6 nM TAX greatly reduced the number of CFU-GMs (Figure 6B; 25.67±7.09 in the TAX-treated group). Similar to CFU-GMs, the number of BFU-Es did not significantly change in the 3 nM BSN-, DSN-, and TAX-treated groups (Figure 6C; 9.67±1.15 in the GLU-treated control group, 9.33±4.04 in the BSN-treated group, 9±1.73 in the DSN-treated group, and 3.67±3.79 in the TAX-treated group), whereas 6 nM TAX greatly reduced the number of BFU-Es (Figure 6C; 0 in the TAX-treated group). When treated with 6 nM DSNs, hematopoietic recovery was clearly seen, indicated by an increased number of myeloid progenitor cells (CFU-GMs) and BFU-Es. The CFU-GMs recovered to almost the same level as the control (Figure 6B; 71±5.57 in the DSN-treated group), and the BFU-Es – though not to the same level as the control – recovered significantly compared with TAX (Figure 6C; 1.33±0.58 in the DSN-treated group and 0 in the TAX-treated group; $P<0.05$). Recovery of CFU-GEMMs could not be clearly seen in the DSN-treated group (Figure 6D; 4.67±1.53 in the GLU-treated control group, 1.33±1.53 in the 3 nM BSN-treated group, 1.00±1.00 in the 3 nM DSN-treated group, 0.33±0.58 in the 3 nM TAX-treated group, 1.33±0.58 in the 6 nM BSN-treated group, and 0 in the 6 nM DSN- and TAX-treated groups). This was not surprising as BSNs greatly reduced the number of CFU-GEMMs, which was very low. When cells were treated with 10 nM DSNs or TAX, no BFU-E or CFU-GEMM colony was observed (data not shown). Taken together, DSNs greatly reduced the myelosuppression toxicity of TAX by promoting proliferation and differentiation of the bone marrow progenitor cells.

Discussion

Although docetaxel (TAX) is one of the most widely used antitumor drugs in clinical chemotherapy to treat several solid cancers, the severe side effects, such as myelosuppression, neutropenia, anemia, and hypersensitivity reaction, and its serious dose-limiting toxicity limit its applications in cancer therapy.[9–11] To improve its side effects while still keep its antitumor activity, new formulations are needed to achieve better clinical applications. In recent decades, nanoscience and nanotechnology has been used in the biomedical field, and they have greatly promoted the development of pharmacy.

Until now, many nanoformulations of docetaxel have been developed.[16,18,24] Compared with other nanoformulations, solid lipid nanoparticles exhibit many advantages, including easier preparation, better stability, and component material safety.[16,29,30,39] The authors have developed novel DSNs using a very simple and convenient method to systemically analyze the toxicity.[29] These newly developed DSNs can increase the maximum tolerated dose of docetaxel and reduce its inherent toxicity.[29]

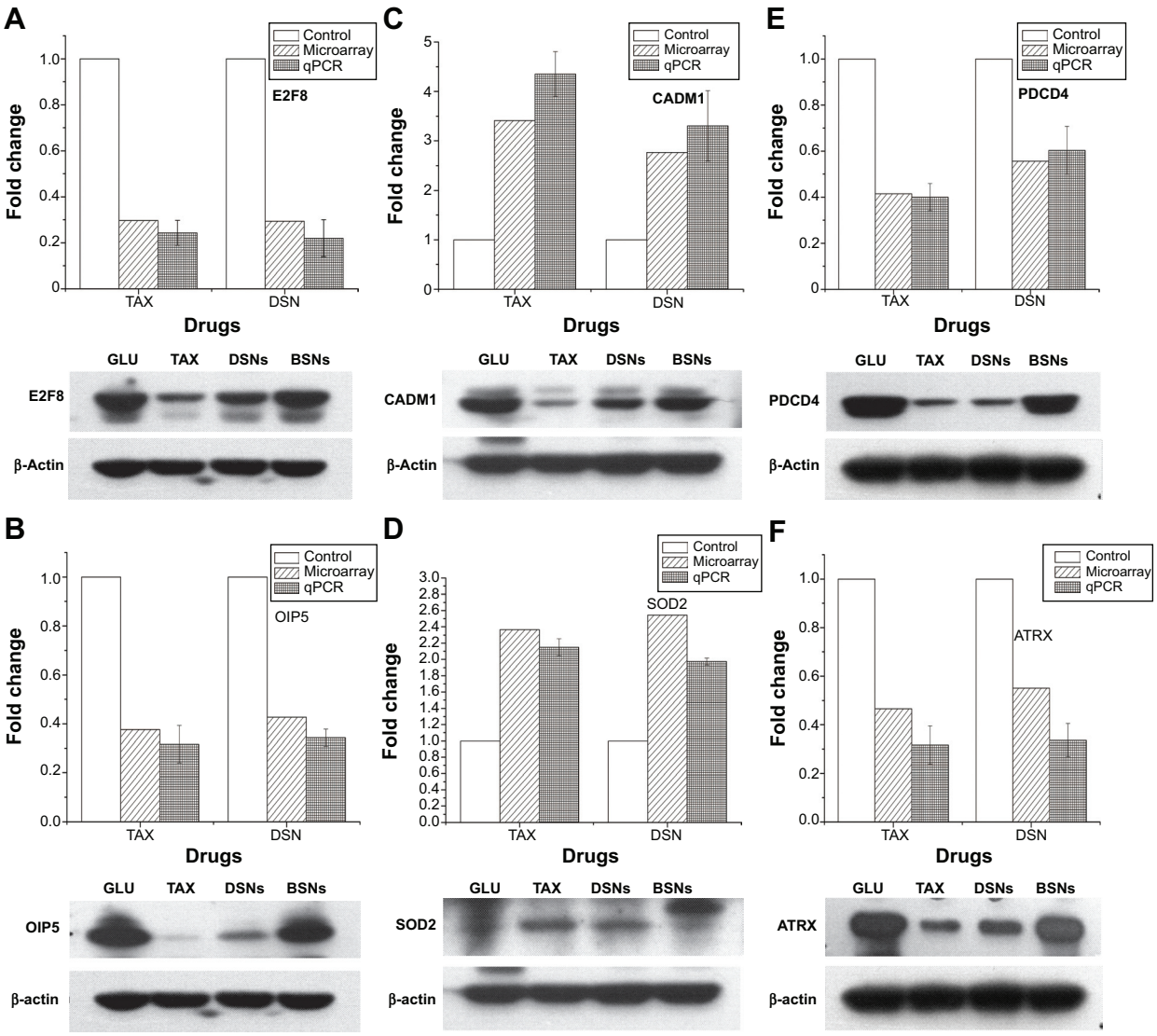

Figure 5 Genes regulated by Taxotere® and docetaxel-loaded solid lipid nanoparticles were confirmed by quantitative polymerase chain reaction and immunoblotting.
Notes: Cell cycle-related genes of E2F8 (**A**) and OIP5 (**B**), proliferation-related genes of NASP (**C**) and SOD2 (**D**), and apoptosis-related genes of PDCD4 (**E**) and PIK3R2 (**F**) were chosen for detection by quantitative polymerase chain reaction and immunoblotting. In quantitative polymerase chain reaction detection, mock-treated cells were set as the control and samples were normalized with the control. In immunoblotting detection, β-actin was used as the loading control.
Abbreviations: BSN, blank solid lipid nanoparticle; DSN, docetaxel-loaded solid lipid nanoparticle; GLU, glucose; qPCR, quantitative polymerase chain reaction; TAX, Taxotere.

Previous studies have shown that docetaxel suppresses the growth of breast cancer MCF-7 cells.[7,8] In this study, MCF-7 breast cancer cells were used to evaluate the tumor suppression activity and myelosuppression toxicity of DSNs. Compared with TAX, DSNs showed lower toxicity at a low dose (eg, 2 nM in 72 hours) in culture cells. While DSNs still keep the antitumor activity of docetaxel, such as inhibiting cell growth, arresting cell cycle progression in the G2/M stage, and inducing apoptosis, it can induce more apoptosis when treated for 24 hours at the 5 nM dose. The in vivo experiments in tumor-bearing nude mice also proved that DSNs and TAX have almost the same antitumor effect.

While the antitumor mechanisms of TAX have been studied before, it is not yet known whether the nano-based DSNs work the same way. To understand the intrinsic mechanisms of DSNs, systemic analysis was performed using microarray to detect gene transcription and then verified with qPCR and immunoblotting. DSN treatment can cause the up- and downregulation of genes similar to TAX, as seen by the large group of common genes shared by both TAX and DSNs.

Myelosuppression is the main side effect of TAX in clinical application; DSNs significantly reduced myelosuppression toxicity compared with TAX when tested in beagle dogs.[29] As myelosuppression is closely related with the proliferation

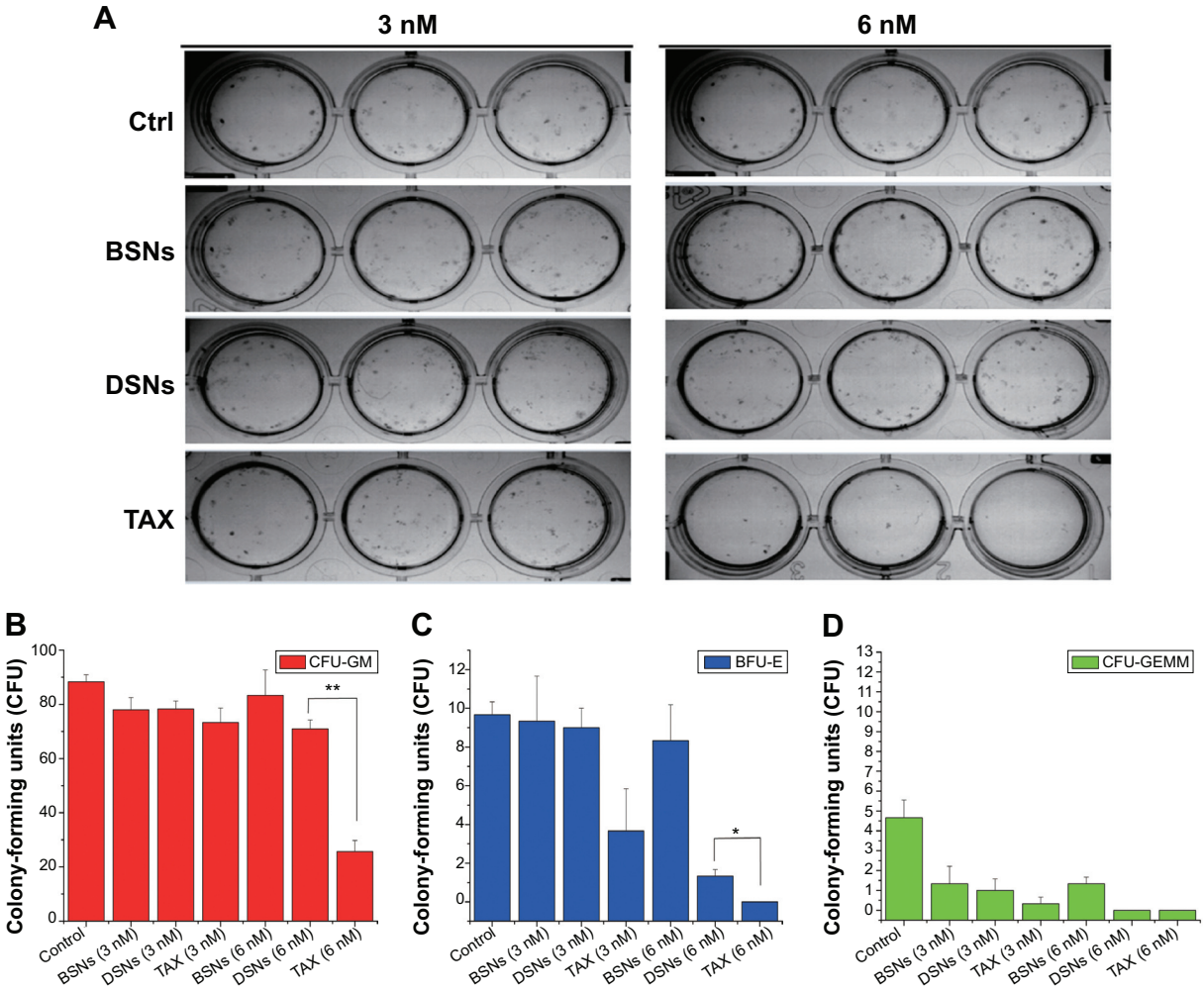

Figure 6 The hematopoietic recovery effect of docetaxel-loaded solid lipid nanoparticles.

Notes: Bone marrow cells from mice were incubated with blank solid lipid nanoparticles, docetaxel-loaded solid lipid nanoparticles, or Taxotere® at 3 nM or 6 nM for 9 days in methylcellulose-based media. Mock-treated cells were used as the control. Optical photos show the microscopic colonies that formed in a 24-well plate (**A**). Colonies of colony forming units that generate granulocytes and macrophages (**B**), burst-forming units that generate erythroids (**C**), and colony forming units that generate granulocytes, erythroids, macrophages, and megakaryocytes (**D**) were counted using an inverted microscope. The data are presented as mean ± standard error from three experiments. *$P<0.05$. **$P<0.01$.

Abbreviations: BFU-E, burst-forming units that generate erythroids; BSN, blank solid lipid nanoparticle; Ctrl, control; CFU-GEMM, colony forming units that generate granulocytes, erythroids, macrophages, and megakaryocytes; CFU-GM, colony forming units that generate granulocytes and macrophages; DSN, docetaxel-loaded solid lipid nanoparticle; TAX, Taxotere.

and differentiation of bone marrow cells, a hematopoietic CFC assay was performed to investigate whether DSNs reduce myelosuppression for improved proliferation and differentiation of bone marrow cells. The results confirmed this possibility and proved that DSNs have more potential in clinical therapy.

Conclusion

The DSNs reduced cytotoxicity, arrested cell cycle progression in the G2/M stage, and induced more apoptosis in MCF-7 cells at a low dose compared with TAX. DSNs and TAX have almost equal antitumor efficacy in tumor-bearing mice. Genes regulated by DSNs and TAX have functions in cell proliferation, apoptosis, and cell cycle control. DSN- and TAX-upregulated or downregulated genes mostly overlap; these genes have functions in DNA replication, DNA damage response, the cytoskeleton, and the cell cycle. Lastly, DSNs greatly reduce myelosuppression toxicity by recovering the proliferation and differentiation of bone marrow progenitor cells.

Acknowledgments

This work was supported by grants from National Basic Research Program of China (973 Program grant no 2010CB934004 and no 2010CB934003), National Natural Science Foundation of China (grant no 31271480), Program of Changjiang Scholar and Innovative Research Team in University (IRT13049), and CAS Knowledge Innovation Program to XB.

Author contributions

QY, WC, YL, and XB designed the study. QY, WC, DM, JH, and ZD performed the experiments. QY, YG, YL, and XB analyzed the data and wrote the manuscript. All authors contributed toward data analysis, drafting and revising the paper and agree to be accountable for all aspects of the work.

Disclosure

The authors report no conflicts of interest in this work.

References

1. Gueritte-Voegelein F, Guenard D, Dubois J, Wahl A, Potier P. [Chemical and biological studies on Taxol (paclitaxel) and Taxotere (docetaxel), new antineoplastic agents]. *J Pharm Belg*. 1994;49(3):193–205. French.
2. Montero A, Fossella F, Hortobagyi G, Valero V. Docetaxel for treatment of solid tumours: a systematic review of clinical data. *Lancet Oncol*. 2005;6(4):229–239.
3. Saloustros E, Georgoulias V. Docetaxel in the treatment of advanced non-small-cell lung cancer. *Expert Rev Anticancer Ther*. 2008; 8(8):1207–1222.
4. Saloustros E, Mavroudis D, Georgoulias V. Paclitaxel and docetaxel in the treatment of breast cancer. *Expert Opin Pharmacother*. 2008; 9(15):2603–2616.
5. Aapro M. The scientific rationale for developing taxoids. *Anticancer Drugs*. 1996;7(Suppl 2):33–36.
6. Canales A, Rodriguez-Salarichs J, Trigili C, et al. Insights into the interaction of discodermolide and docetaxel with tubulin. Mapping the binding sites of microtubule-stabilizing agents by using an integrated NMR and computational approach. *ACS Chem Biol*. 2011;6(8):789–799.
7. Hernandez-Vargas H, Palacios J, Moreno-Bueno G. Molecular profiling of docetaxel cytotoxicity in breast cancer cells: uncoupling of aberrant mitosis and apoptosis. *Oncogene*. 2007;26(20):2902–2913.
8. Berchem GJ, Bosseler M, Mine N, Avalosse B. Nanomolar range docetaxel treatment sensitizes MCF-7 cells to chemotherapy induced apoptosis, induces G2M arrest, and phosphorylates bcl-2. *Anticancer Res*. 1999;19(1A):535–540.
9. Kuppens IE. Current state of the art of new tubulin inhibitors in the clinic. *Curr Clin Pharmacol*. 2006;1(1):57–70.
10. Baker J, Ajani J, Scotte F, et al. Docetaxel-related side effects and their management. *Eur J Oncol Nurs*. 2009;13(1):49–59.
11. Katsumata N. Docetaxel: an alternative taxane in ovarian cancer. *Br J Cancer*. 2003;89(Suppl 3):S9–S15.
12. Hennenfent KL, Govindan R. Novel formulations of taxanes: a review. Old wine in a new bottle? *Ann Oncol*. 2006;17(5):735–749.
13. Weiszhar Z, Czucz J, Revesz C, Rosivall L, Szebeni J, Rozsnyay Z. Complement activation by polyethoxylated pharmaceutical surfactants: Cremophor-EL, Tween-80, and Tween-20. *Eur J Pharm Sci*. 2012; 45(4):492–498.
14. Karve S, Werner ME, Sukumar R, et al. Revival of the abandoned therapeutic wortmannin by nanoparticle drug delivery. *Proc Natl Acad Sci U S A*. 2012;109(21):8230–8235.
15. Hwang HY, Kim IS, Kwon IC, Kim YH. Tumor targetability and antitumor effect of docetaxel-loaded hydrophobically modified glycol chitosan nanoparticles. *J Control Release*. 2008;128(1): 23–31.
16. Xu Z, Chen L, Gu W, et al. The performance of docetaxel-loaded solid lipid nanoparticles targeted to hepatocellular carcinoma. *Biomaterials*. 2009;30(2):226–232.
17. Esmaeili F, Dinarvand R, Ghahremani MH, Ostad SN, Esmaily H, Atyabi F. Cellular cytotoxicity and in-vivo biodistribution of docetaxel poly(lactide-co-glycolide) nanoparticles. *Anticancer Drugs*. 2010; 21(1):43–52.
18. Yanasarn N, Sloat BR, Cui Z. Nanoparticles engineered from lecithin-in-water emulsions as a potential delivery system for docetaxel. *Int J Pharm*. 2009;379(1):174–180.
19. Immordino ML, Brusa P, Arpicco S, Stella B, Dosio F, Cattel L. Preparation, characterization, cytotoxicity, and pharmacokinetics of liposomes containing docetaxel. *J Control Release*. 2003;91(3):417–429.
20. Liang G, Jia-Bi Z, Fei X, Bin N. Preparation, characterization, and pharmacokinetics of N-palmitoyl chitosan anchored docetaxel liposomes. *J Pharm Pharmacol*. 2007;59(5):661–667.
21. Zhai G, Wu J, Xiang G, et al. Preparation, characterization, and pharmacokinetics of folate receptor-targeted liposomes for docetaxel delivery. *J Nanosci Nanotechnol*. 2009;9(3):2155–2161.
22. Werner ME, Copp JA, Karve S, et al. Folate-targeted polymeric nanoparticle formulation of docetaxel is an effective molecularly targeted radiosensitizer with efficacy dependent on the timing of radiotherapy. *ACS Nano*. 2011;5(11):8990–8998.
23. Elsabahy M, Perron ME, Bertrand N, Yu GE, Leroux JC. Solubilization of docetaxel in poly(ethylene oxide)-block-poly(butylene/styrene oxide) micelles. *Biomacromolecules*. 2007;8(7):2250–2257.
24. Shin HC, Alani AW, Rao DA, Rockich NC, Kwon GS. Multi-drug loaded polymeric micelles for simultaneous delivery of poorly soluble anticancer drugs. *J Control Release*. 2009;140(3):294–300.
25. Mu CF, Balakrishnan P, Cui FD, et al. The effects of mixed MPEG-PLA/Pluronic copolymer micelles on the bioavailability and multidrug resistance of docetaxel. *Biomaterials*. 2010;31(8):2371–2379.
26. Liu J, Zahedi P, Zeng F, Allen C. Nano-sized assemblies of a PEG-docetaxel conjugate as a formulation strategy for docetaxel. *J Pharm Sci*. 2008;97(8):3274–3290.
27. Farokhzad OC, Cheng J, Teply BA, et al. Targeted nanoparticle-aptamer bioconjugates for cancer chemotherapy in vivo. *Proc Natl Acad Sci U S A*. 2006;103(16):6315–6320.
28. Zheng D, Li D, Lu X, Feng Z. Enhanced antitumor efficiency of docetaxel-loaded nanoparticles in a human ovarian xenograft model with lower systemic toxicities by intratumoral delivery. *Oncol Rep*. 2010;23(3):717–724.
29. Gao Y, Yang R, Zhang Z, Chen L, Sun Z, Li Y. Solid lipid nanoparticles reduce systemic toxicity of docetaxel: performance and mechanism in animal. *Nanotoxicology*. 2011;5(4):636–649.
30. Zhang P, Chen L, Zhang Z, Lin L, Li Y. Pharmacokinetics in rats and efficacy in murine ovarian cancer model for solid lipid nanoparticles loading docetaxel. *J Nanosci Nanotechnol*. 2010;10(11):7541–7544.
31. Jemal A, Bray F, Center MM, Ferlay J, Ward E, Forman D. Global cancer statistics. *CA Cancer J Clin*. 2011;61(2):69–90.
32. Ferlay J, Shin HR, Bray F, Forman D, Mathers C, Parkin DM. Estimates of worldwide burden of cancer in 2008: GLOBOCAN 2008. *Int J Cancer*. 2010;127(12):2893–2917.
33. Crown J, O'Leary M, Ooi WS. Docetaxel and paclitaxel in the treatment of breast cancer: a review of clinical experience. *Oncologist*. 2004;9(Suppl 2):24–32.
34. Sandberg R, Larsson O. Improved precision and accuracy for microarrays using updated probe set definitions. *BMC Bioinformatics*. 2007;8:48.
35. Smyth GK. Linear models and empirical Bayes methods for assessing differential expression in microarray experiments. *Stat Appl Genet Mol Biol*. 2004;3:Article3.
36. Dennis G Jr, Sherman BT, Hosack DA, et al. DAVID: Database for Annotation, Visualization, and Integrated Discovery. *Genome Biol*. 2003;4(5):P3.
37. Kong L, Yuan Q, Zhu H, et al. The suppression of prostate LNCaP cancer cells growth by selenium nanoparticles through Akt/Mdm2/AR controlled apoptosis. *Biomaterials*. 2011;32(27):6515–6522.
38. Song H, Vita M, Sallam H, et al. Effect of the Cdk-inhibitor roscovitine on mouse hematopoietic progenitors in vivo and in vitro. *Cancer Chemother Pharmacol*. 2007;60(6):841–849.
39. Puri A, Loomis K, Smith B, et al. Lipid-based nanoparticles as pharmaceutical drug carriers: from concepts to clinic. *Crit Rev Ther Drug Carrier Syst*. 2009;26(6):523–580.

Supplementary materials

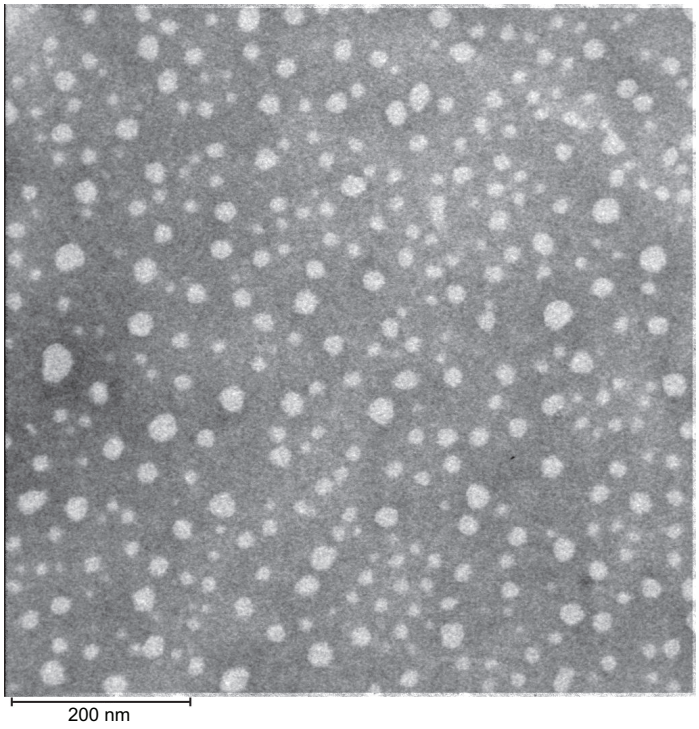

Figure S1 The morphology of docetaxel-loaded solid lipid nanoparticles observed by transmission electron microscopy.
Note: Scale bar = 200 nm.

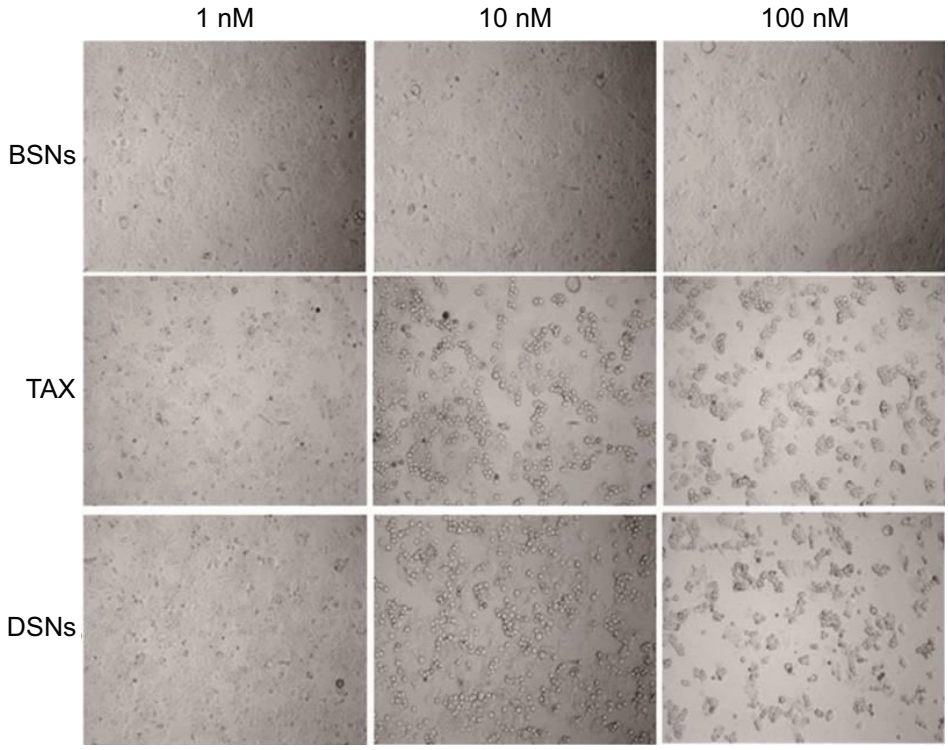

Figure S2 Cell morphology was evaluated under light microscopy after docetaxel-loaded solid lipid nanoparticle and Taxotere® treatment.
Notes: MCF-7 cells were treated with 0–100 nM of docetaxel-loaded solid lipid nanoparticles or Taxotere for 48 hours, then cell morphology was observed under light microscopy and photos were taken under a 10× lens. Blank solid lipid nanoparticles were used as the control.
Abbreviations: BSN, blank solid lipid nanoparticle; DSN, docetaxel-loaded solid lipid nanoparticle; TAX, Taxotere.

Table S3 Primers used for quantitative polymerase chain reaction

Primers	Sequence 5′–3′	Base
H-GLS-F	AGGGTCTGTTACCTAGCTTGG	21
H-GLS-R	ACGTTCGCAATCCTGTAGATTT	22
H-MAF-F	CTGGCAATGAGCAACTCCGA	20
H-MAF-R	AGCCGGTCATCCAGTAGTAGT	21
H-BCL2L11-F	AAACCAACAAGACCCAGCAC	20
H-BCL2L11-R	CGGTGTCTTCTGAAACGTCA	20
H-EHMT1-F	ACTAACTCGGATAGCGGAAAATG	23
H-EHMT1-R	CCAGGAAGGGTTTTTGCAGC	20
H-PIK3R2-F	AAAGGCGGGAACAATAAGCTG	21
H-PIK3R2-R	CAACGGAGCAGAAGGTGAGTG	21
H-GADD45A-F	TGCGAGAACGACATCAACAT	20
H-GADD45A-R	TCCCGGCAAAAACAAATAAG	20
H-C6orf108-F	CTGTACGAGCGGATCGTGTC	20
H-C6orf108-R	TCATAGCCTACACCCAAGGATG	22
H-CADM1-F	GACGTGACAGTGATCGAGGG	20
H-CADM1-R	GGGATCGGTATAGAGCTGGCA	21
H-MKI67-F	GCCTGCTCGACCCTACAGA	19
H-MKI67-R	GCTTGTCAACTGCGGTTGC	19
H-OIP5-F	TGAGAGGGCGATTGACCAAG	20
H-OIP5-R	AGCACTGCGTGACACTGTG	19
H-FZD10-F	GGCGGTGAAGACCATCCTG	19
H-FZD10-R	CAGCTTGTCCGTGTTCTCG	19
H-E2F8-F	CCTGAGATCCGCAACAGAGAT	21
H-E2F8-R	AGATGTCATTATTCACAGCAGGG	23
H-ERBB3-F	GACCCAGGTCTACGATGGGAA	21
H-ERBB3-R	GTGAGCTGAGTCAAGCGGAG	20
H-HOXA13-F	CTCCCGCGCTAAGGAGTTC	19
H-HOXA13-R	CCGGCACCACTGGCATATC	19
H-MCM6-F	TCGGGCCTTGAAAACATTCGT	21
H-MCM6-R	TGTGTCTGGTAGGCAGGTCTT	21
H-MRE11A-F	ATGCAGTCAGAGGAAATGATACG	23
H-MRE11A-R	CAGGCCGATCACCCATACAAT	21
H-NASP-F	GAAAACTATGTGCAAGCTGTGG	22
H-NASP-R	ACTGAGAGTTGTACCCATAAGCC	23
H-SMC1A-F	CATCAAAGCTCGTAACTTCCTCG	23
H-SMC1A-R	CCCCAGAACGACTAATCTCTTCA	23
H-CCNG2-F	TCTGTATTAGCCTTGTGCCTTCT	23
H-CCNG2-R	CCTTGAAACGATCCAAACCAAC	22
H-FAM172A-F	TGAACCGCCTCTTGATTTTCC	21
H-FAM172A-R	AGAGCCTCGTATCTTTTCTGGT	22
H-ATRX-F	GCTGAGCCCATGAGTGAAAG	20
H-ATRX-R	CGTGACGATCCTGAAGACTTG	21
H-IGFBP6-F	TGTGAACCGCAGAGACCAAC	20
H-IGFBP6-R	GCCCATCTCAGTGTCTTGGA	20

(*continued*)

Table S3 (*Continued*)

Primers	Sequence 5′–3′	Base
H-IGFBP3-F	AGACACACTGAATCACCTGAAGT	23
H-IGFBP3-R	AGGGCGACACTGCTTTTTCTT	21
H-MYB-F	ATCTCCCGAATCGAACAGATGT	22
H-MYB-R	TGCTTGGCAATAACAGACCAAC	22
H-SOD2-F	GGAAGCCATCAAACGTGACTT	21
H-SOD2-R	CCCGTTCCTTATTGAAACCAAGC	23
H-PDCD4-F	GGGAGTGACGCCCTTAGAAG	20
H-PDCD4-R	ACCTTTCTTTGGTAGTCCCCTT	22
H-ATF3-F	CAAGTGCATCTTTGCCTCAA	20
H-ATF3-R	CCACCCGAGGTACAGACACT	20
H-β-actin-F	GATGAGATTGGCATGGCTTT	20
H-β-actin-R	CACCTTCACCGTTCCAGTTT	20

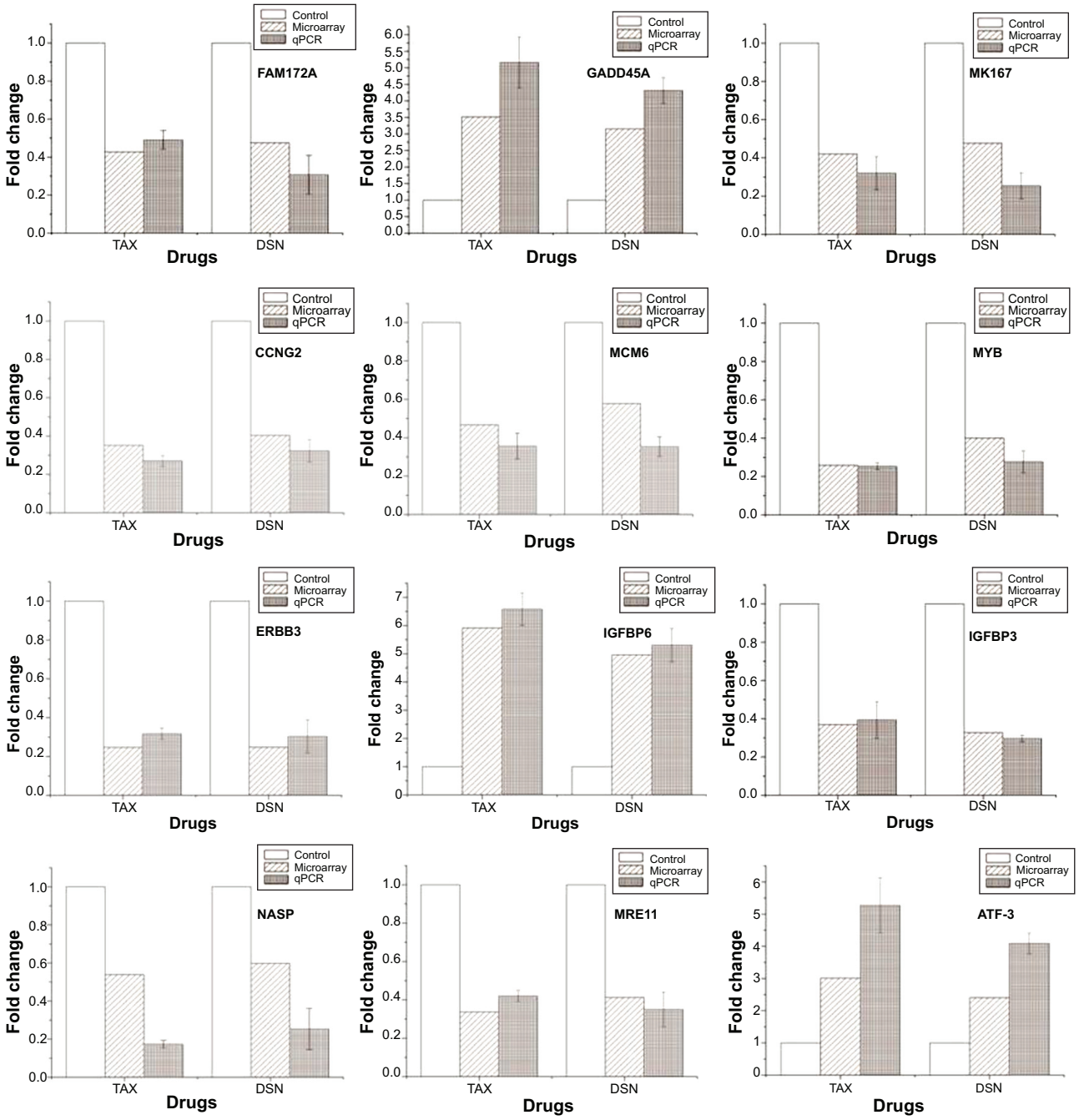

Figure S3 Fold change in transcription after drug treatment of genes involved in cell proliferation, apoptosis, cell cycle regulation, and DNA damage response detected by messenger RNA microarray and quantitative polymerase chain reaction.
Note: The mock-treated sample was set as the control and other samples were normalized with the control.
Abbreviations: DSN, docetaxel-loaded solid lipid nanoparticle; qPCR, quantitative polymerase chain reaction; TAX, Taxotere®.

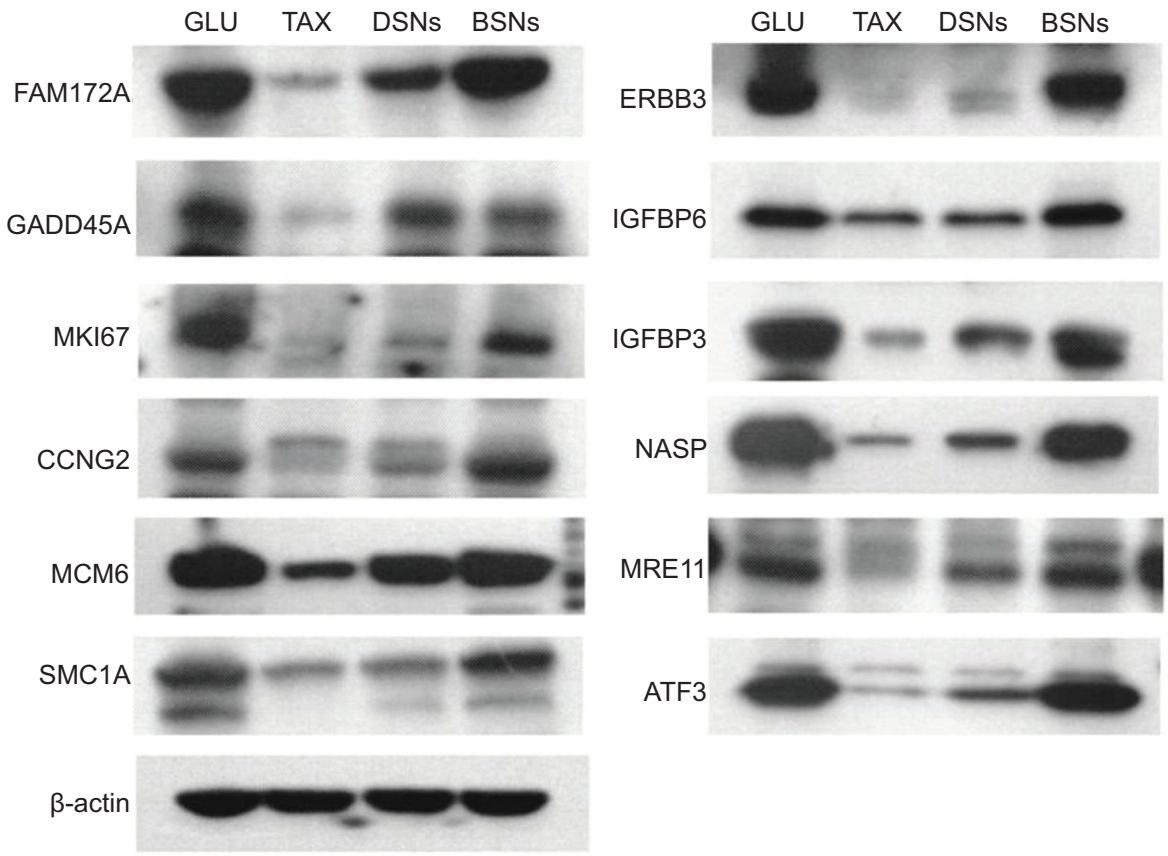

Figure S4 Change in the protein expression of genes involved in cell proliferation, apoptosis, cell cycle regulation, and DNA damage response after drug treatment detected by immunoblotting.
Note: β-actin was used as the loading control.
Abbreviations: BSN, blank solid lipid nanoparticle; DSN, docetaxel-loaded solid lipid nanoparticle; GLU, glucose; TAX, Taxotere®.